

Unsaturation in Binuclear Cyclopentadienyliron Carbonyls

Hongyan Wang,^{†‡} Yaoming Xie,[‡] R. Bruce King,^{*‡} and Henry F. Schaefer III[‡]

Atomic and Molecular Physics Institute, Sichuan University, Chengdu 610065, People's Republic of China, and Department of Chemistry and Center for Computational Chemistry, University of Georgia, Athens, Georgia 30602

Received September 20, 2005

The binuclear cyclopentadienyliron carbonyls $\text{Cp}_2\text{Fe}_2(\text{CO})_n$ ($n = 4, 3, 2, 1$; $\text{Cp} = \eta^5\text{-C}_5\text{H}_5$) have been studied by density functional theory (DFT) using the B3LYP and BP86 methods. The *trans*- and *cis*- $\text{Cp}_2\text{Fe}_2(\text{CO})_2(\mu\text{-CO})_2$ isomers of $\text{Cp}_2\text{Fe}_2(\text{CO})_4$ known experimentally are predicted by DFT methods to be genuine minima with no significant imaginary vibrational frequencies. The energies of these two $\text{Cp}_2\text{Fe}_2(\text{CO})_2(\mu\text{-CO})_2$ structures are very similar, consistent with the experimental observation of an equilibrium between these isomers in solution. An intermediate between the interconversion of the *trans*- and *cis*- $\text{Cp}_2\text{Fe}_2(\text{CO})_2(\mu\text{-CO})_2$ dibridged isomers of $\text{Cp}_2\text{Fe}_2(\text{CO})_4$ can be the *trans* unbridged isomer of $\text{Cp}_2\text{Fe}_2(\text{CO})_4$ calculated to be 2.3 kcal/mol (B3LYP) or 9.1 kcal/mol (BP86) above the global minimum *trans*- $\text{Cp}_2\text{Fe}_2(\text{CO})_2(\mu\text{-CO})_2$. For the unsaturated $\text{Cp}_2\text{Fe}_2(\text{CO})_3$, the known triplet isomer $\text{Cp}_2\text{Fe}_2(\mu\text{-CO})_3$ with an Fe=Fe double bond similar to the O=O double bond in O_2 is found to be the global minimum. The lowest-energy structure for the even more unsaturated $\text{Cp}_2\text{Fe}_2(\text{CO})_2$ is a dibridged structure $\text{Cp}_2\text{Fe}_2(\mu\text{-CO})_2$, with a short Fe–Fe distance suggestive of the Fe≡Fe triple bond required to give both Fe atoms the favored 18-electron configuration. Singlet and triplet unbridged structures for $\text{Cp}_2\text{Fe}_2(\text{CO})_2$ were also found but at energies considerably higher (20–50 kcal/mol) than that of the global minimum $\text{Cp}_2\text{Fe}_2(\mu\text{-CO})_2$. The lowest-energy structure for $\text{Cp}_2\text{Fe}_2(\text{CO})$ is the triplet unsymmetrically bridged structure $\text{Cp}_2\text{Fe}_2(\mu\text{-CO})$, with a short Fe–Fe distance (~ 2.1 Å) suggestive of the $\sigma + 2\pi + \frac{1}{2}\delta$ Fe⁴–Fe quadruple bond required to give both Fe atoms the favored 18-electron rare gas configuration.

1. Introduction

The chemistry of cyclopentadienyliron carbonyls dates back approximately 50 years to the synthesis of $(\eta^5\text{-C}_5\text{H}_5)_2\text{Fe}_2(\text{CO})_4$ (**1** in Figure 1) by Piper and Wilkinson in 1956.¹ Since then, **1**, which is readily available by simply heating $\text{Fe}(\text{CO})_5$ with a cyclopentadiene dimer to about 130 °C, has become one of the more important starting materials for the synthesis of diverse types of significant organoiron compounds.

The correct distribution of terminal and bridging CO groups in **1**, namely, $(\eta^5\text{-C}_5\text{H}_5)_2\text{Fe}_2(\text{CO})_2(\mu\text{-CO})_2$, was originally deduced from its infrared $\nu(\text{CO})$ frequencies and then subsequently confirmed by X-ray and neutron diffraction studies.^{2–4} These structural studies showed that **1**, as the *trans*

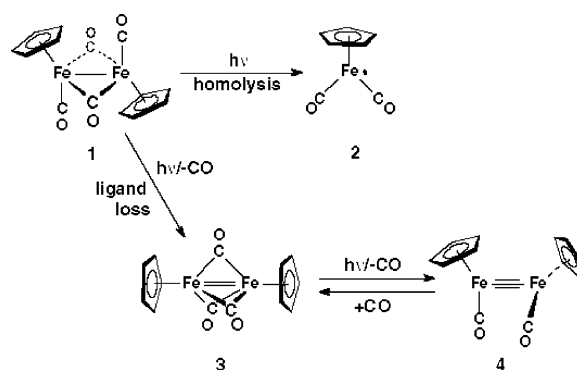


Figure 1. Two reaction channels in the photolysis of $(\eta^5\text{-C}_5\text{H}_5)_2\text{Fe}_2(\text{CO})_2(\mu\text{-CO})_2$.

isomer, has a centrosymmetric structure in the solid phase with two bridging and two terminal CO groups and an Fe–Fe distance of 2.54 Å, consistent with an Fe–Fe single bond. Subsequent low-temperature crystallization studies led

* To whom correspondence should be addressed. E-mail: rbking@sunchem.chem.uga.edu.

[†] Sichuan University.

[‡] University of Georgia.

(1) Piper, T. S.; Wilkinson, G. *J. Inorg. Nucl. Chem.* **1956**, *6*, 104.

(2) Mills, O. S. *Acta Crystallogr.* **1958**, *11*, 620.

(3) Bryan, R. F.; Greene, P. T. *J. Chem. Soc. A* **1970**, 3068.

(4) Mitschler, A.; Rees, B.; Lehmann, M. S. *J. Am. Chem. Soc.* **1978**, *100*, 3390.

to the isolation of the corresponding cis dibridged isomer.⁵ In addition, infrared spectra of **1** in various solvents showed that not only bridged but also nonbridged isomers are present.^{6–8} Thus, three isomers of **1** in equilibrium were detected in various solvents, namely, the trans and cis dibridged isomers, as well as a small amount of an unbridged isomer. The cis–trans ratio between the two bridged isomers ($(\eta^5\text{-C}_5\text{H}_5)_2\text{Fe}_2(\text{CO})_2(\mu\text{-CO})_2$) was found to depend on the solvent polarity, with the trans form predominating in nonpolar solvents and the cis form dominating in polar solvents.⁶ The cis–trans ratio of ($\eta^5\text{-C}_5\text{H}_5$)₂Fe₂(CO)₂($\mu\text{-CO}$)₂ was found to be essentially temperature-independent, suggesting approximately equal enthalpies of formation for both isomers. Only minuscule amounts (<1%) of an unbridged isomer of **1** were detected in solution by infrared spectroscopy.⁷

Photolysis of **1** leads to two different reaction channels (Figure 1), namely, homolysis of the Fe–Fe bond to form two ($\eta^5\text{-C}_5\text{H}_5$)Fe(CO)₂[•] radicals (**2** in Figure 1)^{9,10} and loss of a carbonyl group with retention of the Fe–Fe bond to give the unsaturated derivative ($\eta^5\text{-C}_5\text{H}_5$)₂Fe₂($\mu\text{-CO}$)₃ (**3** in Figure 1) with a formal Fe=Fe double bond.^{11–13} The permethylated derivative of **3**, namely, ($\eta^5\text{-Me}_5\text{C}_5$)₂Fe₂($\mu\text{-CO}$)₃, has been isolated in the pure state and shown by X-ray diffraction to have three bridging CO groups and an Fe–Fe distance of 2.265 Å, consistent with the Fe=Fe formal double bond required to give each Fe atom an 18-electron rare gas configuration.¹⁴ The paramagnetism of ($\eta^5\text{-Me}_5\text{C}_5$)₂Fe₂($\mu\text{-CO}$)₃ indicates a triplet state, so that its Fe=Fe double bond is an analogue of the O=O double bond in triplet O₂ rather than the C=C double bond in singlet ethylene. Intermediates proposed in the photochemical formation of **3** from **1** include ($\eta^5\text{-C}_5\text{H}_5$)₂Fe₂(CO)₃ with all terminal CO groups, ($\eta^5\text{-C}_5\text{H}_5$)₂Fe₂(CO)($\mu\text{-CO}$)₂ with two bridging CO groups, and ($\eta^5\text{-C}_5\text{H}_5$)₂Fe₂($\mu, \eta^1, \eta^2\text{-CO}$)($\mu\text{-CO}$)₂ with a four-electron donor bridging CO group bonded to one of the two Fe atoms through the O atom as well as the C atom.^{14,15}

More recently, Kvietok and Bursten have detected a double-CO loss photoproduct¹⁶ ($\eta^5\text{-C}_5\text{H}_5$)₂Fe₂(CO)₂ from the matrix photolysis of ($\eta^5\text{-C}_5\text{H}_5$)₂Fe₂(CO)₂($\mu\text{-CO}$)₂. A C₂ structure (**4** in Figure 1) with an unsupported Fe≡Fe triple bond was suggested¹⁷ for this photoproduct based on the

observation of two terminal $\nu(\text{CO})$ frequencies of approximately equal intensities as well as the absence of bridging $\nu(\text{CO})$ frequencies. A similar unsaturated species ($\eta^5\text{-C}_5\text{H}_5$)₂Fe₂(CO)₂ is a likely intermediate in the preparation of the very stable tetramer ($\eta^5\text{-C}_5\text{H}_5$)₄Fe₄(CO)₄ by the pyrolysis of ($\eta^5\text{-C}_5\text{H}_5$)₂Fe₂(CO)₂($\mu\text{-CO}$)₂ in a solvent such as toluene.¹⁸ No evidence has been found experimentally for even more highly unsaturated cyclopentadienyliron carbonyls of stoichiometry ($\eta^5\text{-C}_5\text{H}_5$)₂Fe₂(CO), where an Fe⁴–Fe quadruple bond is required to give each Fe atom the favored 18-electron rare gas configuration if the single CO group is a normal two-electron donor.

This paper examines possible structures for the cyclopentadienyliron carbonyls ($\eta^5\text{-C}_5\text{H}_5$)₂Fe₂(CO)_{*n*} (*n* = 4, 3, 2, and 1) using density functional theory (DFT) methods, with the objective of interpreting known experimental information as well as predicting new structures.

2. Computational Methods

DFT methods, which attempt to include electron correlation effects, have been widely described to be a practical and effective computational tool, especially for organometallic compounds. Among DFT procedures, the most reliable approximation is often thought to be the hybrid Hartree–Fock (HF)/DFT method using a combination of the three-parameter Becke exchange functional with the Lee–Yang–Parr nonlocal correlation functional known as B3LYP.^{19,20} However, another DFT method, which combines Becke’s 1988 exchange functional with Perdew’s 1986 nonlocal correlation functional method (BP86),^{21,22} was also used in the present paper for comparison.

Basis sets have been chosen to provide continuity with a body of existing research on organometallic compounds. Fortunately, DFT methods are far less sensitive to basis sets than higher level methods such as coupled cluster theory. In this work, the double- ζ plus polarization (DZP) basis sets used for C and O add one set of pure spherical harmonic d functions with orbital exponents $\alpha_d(\text{C}) = 0.75$ and $\alpha_d(\text{O}) = 0.85$ to the Huzinaga–Dunning standard contracted DZ sets^{23,24} and are designated as 9s5p1d/4s2p1d. For H, a set of p polarization functions $\alpha_p(\text{H}) = 0.75$ is added to the Huzinaga–Dunning DZ set. For Fe, in our loosely contracted DZP basis set, Wachters’ primitive set is used but augmented by two sets of p functions and one set of d functions, contracted following Hood et al., and designated as 14s11p6d/10s8p3d.²⁵

All possible structures, i.e., dibridged cis and trans isomers as well as nonbridged cis and trans isomers for the various Cp₂Fe₂(CO)_{*n*} (*n* = 4, 3, 2, 1) derivatives (Cp = $\eta^5\text{-C}_5\text{H}_5$), were optimized using the DZP B3LYP and DZP BP86 methods. The vibrational frequencies were also obtained at the same levels by evaluating analytically the second derivatives of the energy with respect to the nuclear coordinates. The corresponding infrared intensities were evaluated analytically as well. All of the computations were performed using the *Gaussian 94* program,²⁶ in which the fine grid (75, 302) is the default for evaluating integrals numerically and

- (5) Bryan, R. F.; Greene, P. T.; Newlands, M. J.; Field, D. S. *J. Chem. Soc. A* **1970**, 3068.
 (6) Manning, A. R. *J. Chem. Soc. A* **1968**, 1319.
 (7) Fischer, R. D.; Vogler, A.; Noack, K. *J. Organomet. Chem.* **1967**, *7*, 135.
 (8) Cotton, F. A.; Yagupsky, G. *Inorg. Chem.* **1967**, *6*, 15.
 (9) Abrahamson, H. B.; Palazotto, M. C.; Reichel, C. L.; Wrighton, M. S. *J. Am. Chem. Soc.* **1979**, *101*, 4123.
 (10) Baird, M. C. *Chem. Rev.* **1988**, *88*, 1217.
 (11) Caspar, J. V.; Meyer, T. J. *J. Am. Chem. Soc.* **1980**, *102*, 7794.
 (12) Hooker, R. H.; Mahmoud, K. A.; Rest, A. J. *Chem. Commun.* **1983**, 1022.
 (13) Hepp, A. F.; Blaha, J. P.; Lewis, C.; Wrighton, M. S. *Organometallics* **1984**, *3*, 174.
 (14) Blaha, J. P.; Bursten, B. E.; Dewan, J. C.; Frankel, R. B.; Randolph, C. L.; Wilson, B. A.; Wrighton, M. S. *J. Am. Chem. Soc.* **1985**, *107*, 4561.
 (15) Vitale, M.; Lee, K. K.; Hemann, C. F.; Hille, R.; Gustafson, T. L.; Bursten, B. E. *J. Am. Chem. Soc.* **1995**, *118*, 2286.
 (16) Kvietok, F. A.; Bursten, B. E. *J. Am. Chem. Soc.* **1994**, *116*, 9807.
 (17) Vitale, M.; Archer, M. E.; Bursten, B. E. *Chem. Commun.* **1998**, 179.

- (18) King, R. B. *Inorg. Chem.* **1966**, *5*, 2227.
 (19) Becke, A. D. *J. Chem. Phys.* **1993**, *98*, 5648.
 (20) Lee, C.; Yang, W.; Parr, R. G. *Phys. Rev. B* **1988**, *37*, 785.
 (21) Becke, A. D. *Phys. Rev. A* **1988**, *38*, 3098.
 (22) Perdew, J. P. *Phys. Rev. B* **1986**, *33*, 8822.
 (23) Dunning, T. H. *J. Chem. Phys.* **1970**, *53*, 2823.
 (24) Huzinaga, S. *J. Chem. Phys.* **1965**, *42*, 1293.
 (25) (a) Wachters, A. J. H. *J. Chem. Phys.* **1970**, *52*, 1033. (b) Hood, D. M.; Pitzer, R. M.; Schaefer, H. F. *J. Chem. Phys.* **1979**, *71*, 705.

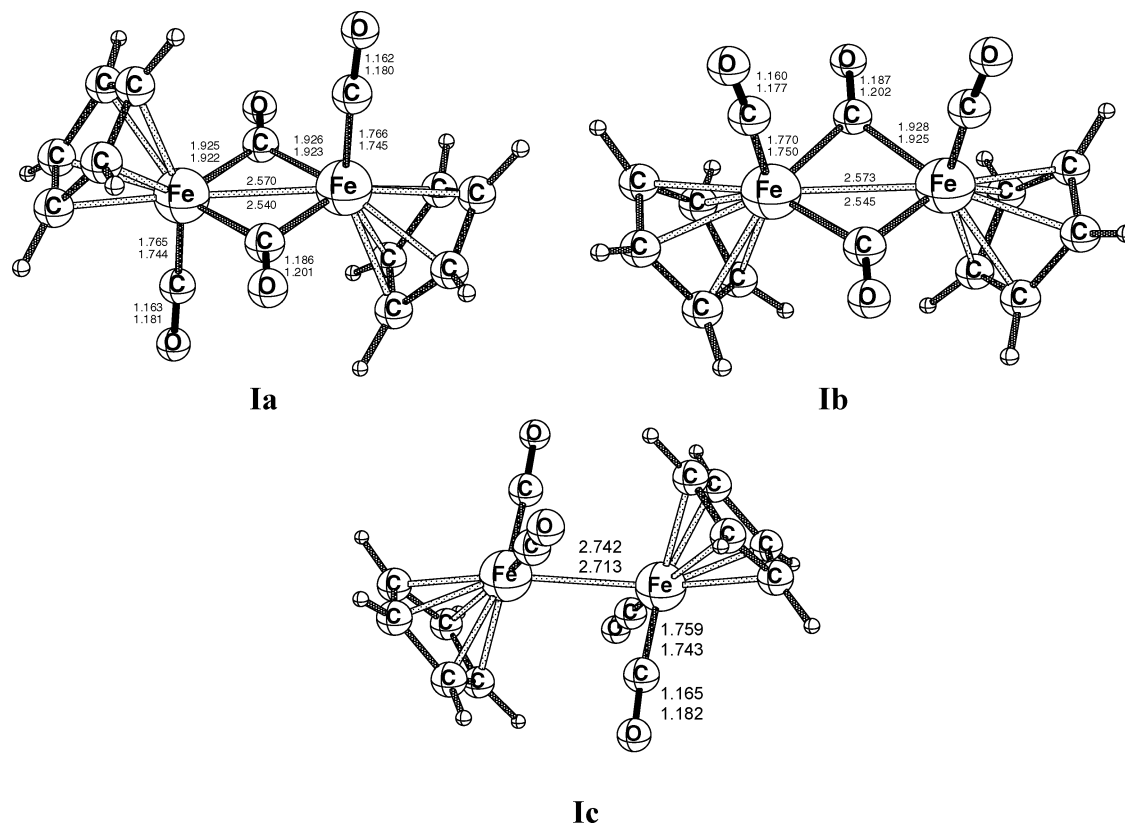


Figure 2. Three optimized isomers of $\text{Cp}_2\text{Fe}_2(\text{CO})_4$.

the tight (10^{-8} hartree) designation is the default for the self-consistent-field convergence.

In the search for minima, low-magnitude imaginary vibrational frequencies are suspicious because the numerical integration procedures used in existing DFT methods have significant limitations. Thus, an imaginary vibrational frequency with a magnitude of less than $100i \text{ cm}^{-1}$ should imply that there is a minimum with energy identical with or close to that of the stationary point in question. In most cases, we do not generally follow the eigenvectors corresponding to imaginary vibrational frequencies of less than $100i \text{ cm}^{-1}$ in search of another minimum.²⁷

The optimized geometries from these computations are depicted in Figures 2–5, with all bond distances given in angstroms.

3. Results and Discussion

3.1. Molecular Structures. 3.1.1. $\text{Cp}_2\text{Fe}_2(\text{CO})_4$. Four possible isomers of $\text{Cp}_2\text{Fe}_2(\text{CO})_4$, namely, dibridged cis and trans isomers as well as unbridged cis and trans isomers, were considered for optimization using the B3LYP and BP86 methods. The optimized structures are shown in Figure 2, and the optimized structural parameters are presented in Table 1. Three stable isomers of $\text{Cp}_2\text{Fe}_2(\text{CO})_4$ were obtained, namely, the C_s trans dibridged isomer **Ia**, the C_{2v} cis

dibridged isomer **Ib**, and the C_{2h} trans unbridged isomer **Ic**. The cis unbridged isomer of $\text{Cp}_2\text{Fe}_2(\text{CO})_4$ is not a stationary point but converts to the trans dibridged stable isomer **Ia** upon optimization.

The trans dibridged isomer **Ia** and trans unbridged isomer **Ic** have real vibrational frequencies, confirming that they are genuine minima of the energy surface. However, the cis dibridged isomer **Ib** is found to have two small imaginary vibrational frequencies of $46i$ and $30i \text{ cm}^{-1}$ (B3LYP) or $53i$ and $36i \text{ cm}^{-1}$ (BP86). Because these imaginary vibrational frequencies are far less than $100i \text{ cm}^{-1}$, the actual minimum is likely to be identical with or close to that of structure **Ib**.²⁷

The energy of the trans unbridged isomer **Ic** is higher than that of the trans dibridged isomer **Ia** by 2.3 kcal/mol (B3LYP) or 9.1 kcal/mol (BP86). Furthermore, the energy of the trans dibridged isomer is lower than that of the cis dibridged isomer by 0.6 kcal/mol (B3LYP) or 1.7 kcal/mol (BP86), in disagreement with solution NMR data. Thus, the proton NMR spectra of $\text{Cp}_2\text{Fe}_2(\text{CO})_4$ in a C_6D_6 – CS_2 solution showed that the cis dibridged isomer is 1.3 kcal/mol more stable than the trans dibridged isomer.¹⁷ However, the computed energy difference between **Ia** and **Ib** is so small that it could be overcome by solvation. The bond distances and angles of **Ia** and **Ib** agree well with experimental data from X-ray diffraction (Table 1).

3.1.2. $\text{Cp}_2\text{Fe}_2(\text{CO})_3$. The lowest-energy structure for $\text{Cp}_2\text{Fe}_2(\text{CO})_3$ found in this research (Table 2) is the tribridged isomer $\text{Cp}_2\text{Fe}_2(\mu\text{-CO})_3$ (**IIa** in Figure 3), which has D_{3h} symmetry of the central $\text{Fe}(\mu\text{-CO})_3\text{Fe}$ core. This isomer is found to be a ground-state triplet and to have only very small

(26) Frisch, M. J.; Trucks, G. W.; Schlegel, H. B.; Gill, P. M. W.; Johnson, B. G.; Robb, M. A.; Cheeseman, J. R.; Keith, T.; Petersson, G. A.; Montgomery, J. A.; Raghavachari, K.; Al-Laham, M. A.; Zakrzewski, V. G.; Ortiz, J. V.; Foresman, J. B.; Peng, C. Y.; Ayala, P. Y.; Chen, W.; Wong, M. W.; Andes, J. L.; Replogle, E. S.; Gomperts, R.; Martin, R. L.; Fox, D. J.; Binkley, J. S.; Defrees, D. J.; Baker, J.; Stewart, J. J. P.; Head-Gordon, M.; Gonzalez, C.; Pople, J. A. *Gaussian 94*, revision B.3; Gaussian Inc.: Pittsburgh, PA, 1995.

(27) Xie, Y.; Schaefer, H. F.; King, R. B. *J. Am. Chem. Soc.* **2000**, *122*, 8746.

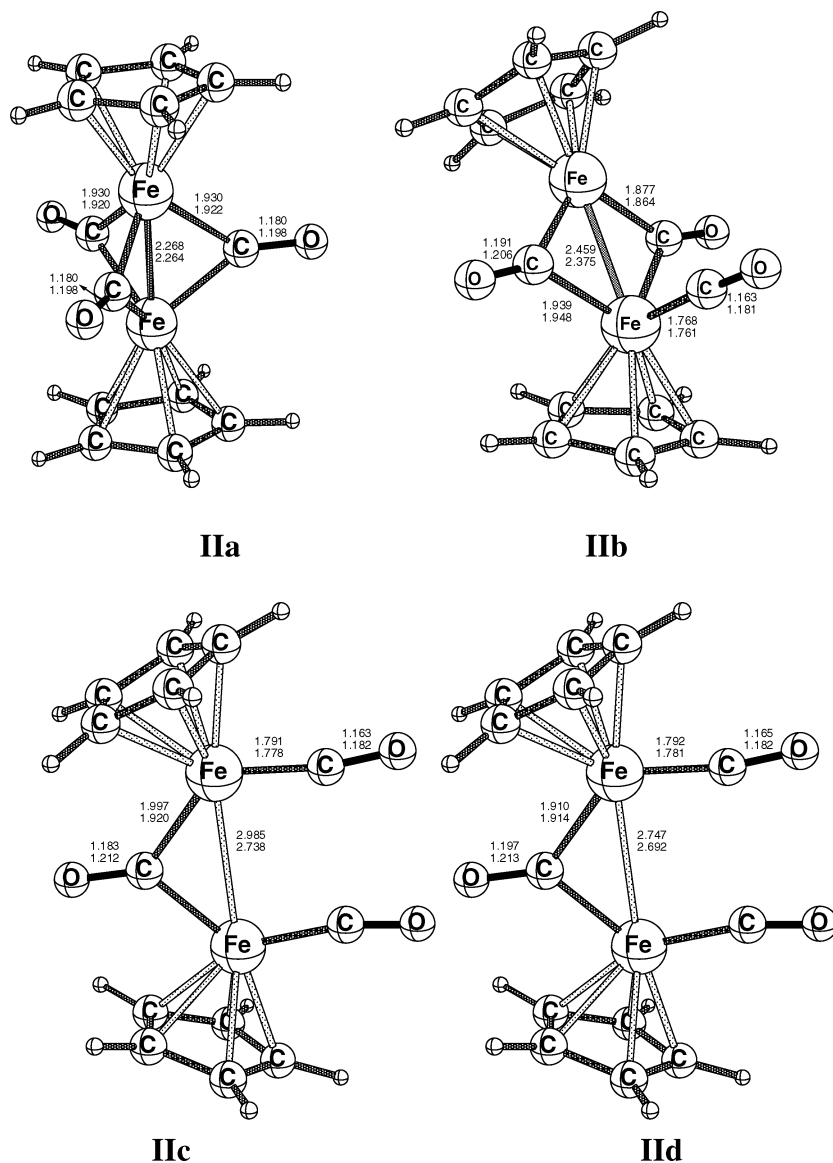


Figure 3. Four optimized isomers of $\text{Cp}_2\text{Fe}_2(\text{CO})_3$.

imaginary vibrational frequencies, namely, $25i$ and $23i$ cm^{-1} (B3LYP) or $25i$ and $24i$ cm^{-1} (BP86). Using a finer (99, 590) grid than the (75, 302) default grid of the *Gaussian 94* program predicts all real vibrational frequencies for the **IIa** structure. A permethylated derivative of **IIa**, namely, $(\eta^5\text{-Me}_5\text{C}_5)_2\text{Fe}_2(\mu\text{-CO})_3$, has been isolated and structurally characterized by X-ray diffraction.¹⁴ The Fe=Fe distance found by X-ray crystallography for $(\eta^5\text{-Me}_5\text{C}_5)_2\text{Fe}_2(\mu\text{-CO})_3$ is 2.265 Å, which is remarkably close to the computed value of 2.268 Å (B3LYP) or 2.264 Å (BP86) for **IIa** (in Table 2). The magnetic properties of $(\eta^5\text{-Me}_5\text{C}_5)_2\text{Fe}_2(\mu\text{-CO})_3$ indicate that it is a triplet consistent with our DFT studies.^{12,13}

An attempt to optimize the analogous singlet tribridged structure leads to a dibridged $\text{Cp}_2\text{Fe}_2(\text{CO})(\mu\text{-CO})_2$ structure (**IIb** in Figure 3) at an energy higher than that of the triplet structure **IIa** by 11.3 kcal/mol (B3LYP) or 10.7 kcal/mol (BP86). Furthermore, **IIb** is a genuine minimum or is close to the genuine minimum because it has small vibrational frequencies, namely, $20i$ cm^{-1} (B3LYP) or $31i$ cm^{-1} (BP86).

The monobridged isomer $\text{Cp}_2\text{Fe}_2(\text{CO})_2(\mu\text{-CO})$ (**II d** in Figure 3) was found to have a singlet electronic ground state at 43.7 kcal/mol (B3LYP) or 44.8 kcal/mol (BP86) above the tribridged global minimum **IIa** (Table 2) with two small imaginary vibrational frequencies of $67i$ and $32i$ cm^{-1} (B3LYP) or $67i$ and 29 cm^{-1} (BP86). Because these imaginary vibrational frequencies are less than $100i$ cm^{-1} , the actual minimum is likely to be identical or close to structure **II d**. The corresponding triplet monobridged isomer **IIc** was found to have large imaginary vibrational frequencies, namely, $786i$ and $602i$ cm^{-1} (B3LYP) or $838i$ cm^{-1} (BP86) after optimization (Table 2). This indicates that **IIc** is a transition state rather than a genuine minimum. Following these large imaginary vibrational frequencies converts structure **IIc** into the tribridged global minimum structure **IIa**. The monobridged isomers **IIc** and **II d** were found to have significantly longer Fe–Fe distances than the tribridged isomers **IIa** and **IIb** by ~ 0.5 Å.

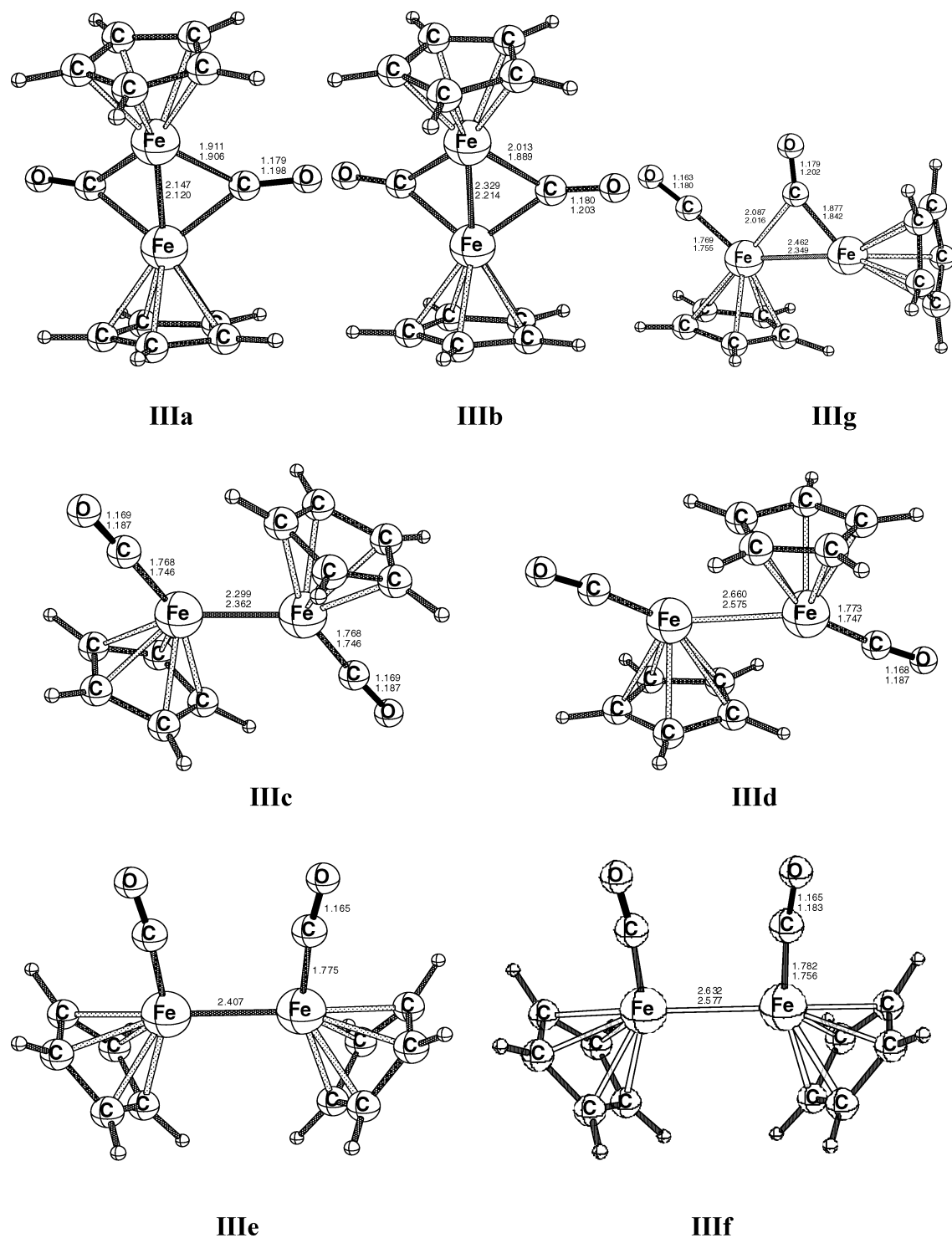


Figure 4. Seven isomers of $\text{Cp}_2\text{Fe}_2(\text{CO})_2$.

3.1.3. $\text{Cp}_2\text{Fe}_2(\text{CO})_2$. Six structures were optimized for $\text{Cp}_2\text{Fe}_2(\text{CO})_2$ (Figure 4 and Table 3), namely, singlet and triplet dibridged structures as well as trans and cis unbridged structures. The results were strongly dependent upon the method used (B3LYP or BP86). Thus, the predicted global minimum for $\text{Cp}_2\text{Fe}_2(\text{CO})_2$ using the BP86 method is the singlet C_{2v} structure **IIIa** with two symmetric bridging CO ligands. The calculated dihedral angle between the two Fe–C(O)–Fe planes in **IIIa** is 136.9° (B3LYP) or 128.5° (BP86), so that **IIIa** can be viewed as derived from **IIa** by the loss

of one of the bridging CO groups. The theoretical Fe–Fe distance in **IIIa** is only 2.147 Å (B3LYP) or 2.120 Å (BP86), consistent with the Fe≡Fe triple bond required to give each Fe atom in **IIIa** the favored 18-electron rare gas configuration.

The predicted global minimum for $\text{Cp}_2\text{Fe}_2(\text{CO})_2$ using the B3LYP method is a triplet dibridged structure $\text{Cp}_2\text{Fe}_2(\mu\text{-CO})_2$ (**IIIb** in Figure 4) rather than the singlet dibridged structure (**IIIa**) found using the BP86 method. Thus, structure **IIIb** is lower in energy than structure **IIIa** by 9.8 kcal/mol using

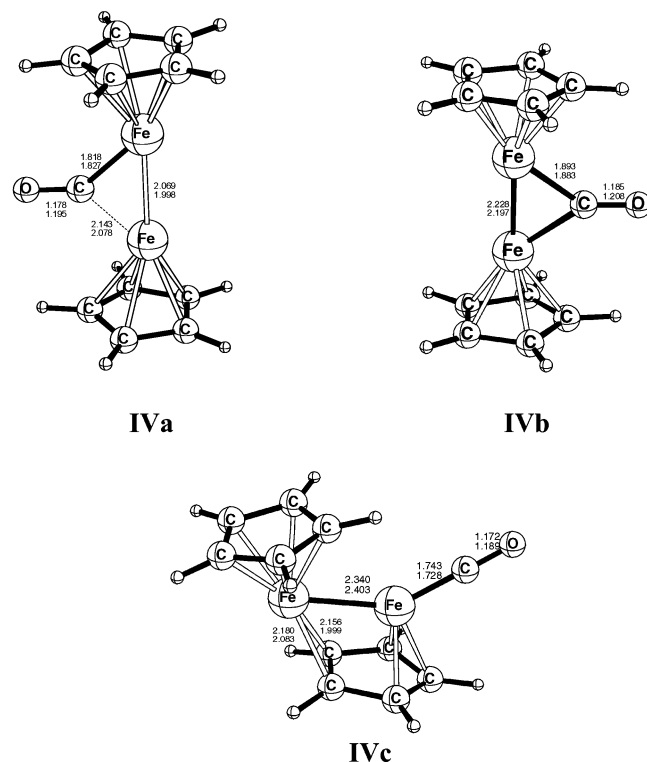


Figure 5. Three isomers of $\text{Cp}_2\text{Fe}_2(\text{CO})$.

the B3LYP method, while it is higher in energy than structure **IIIa** by 3.4 kcal/mol using the BP86 method. The small imaginary frequencies of $91i$ and $35i$ cm^{-1} (B3LYP) or $22i$ cm^{-1} (BP86) calculated for **IIIb** show that the actual minimum is identical with or close to those of structure **IIIb**.

Among the unbridged structures for $\text{Cp}_2\text{Fe}_2(\text{CO})_2$, both the trans and cis singlet unbridged structures, **IIIc** and **IIIe**, have several imaginary vibrational frequencies. Following the mode of the largest imaginary vibrational frequency converts both **IIIc** and **IIIe** into the dibridged global minimum **IIIa**.

The trans and cis triplet unbridged structures are lower in energy than the corresponding singlet structures. Thus, structure **IIId** is lower than **IIIc** by 25.5 kcal/mol (B3LYP) or 5.3 kcal/mol (BP86), and structure **IIIf** is lower than **IIId** by 29.5 kcal/mol. Like the singlet cis unbridged structures **IIIe**, the triplet structure **IIIf** has several imaginary vibra-

tional frequencies. Following the mode of the largest imaginary vibrational frequency ($132i$ cm^{-1}) of **IIIf** leads to a new singly bridged structure **IIIg** (Figure 3). However, **IIIg** has a large imaginary vibrational frequency ($334i$ cm^{-1}) by B3LYP, indicating that it is a transition state rather than a genuine minimum. Following the largest imaginary vibrational frequency ($334i$ cm^{-1}) of structure **IIIg** converts it to structure **IIIb**.

3.1.4. $\text{Cp}_2\text{Fe}_2(\text{CO})$. Optimizations have been carried out on triplet and singlet $\text{Cp}_2\text{Fe}_2(\text{CO})$ structures in which the single CO group is either bridging or terminal. The triplet unbridged structure collapses to the C_1 bridged triplet structure **IVa**, which has by far the lowest energy among the three successfully optimized structures and thus is the global minimum (Figure 5 and Table 4). The bridging CO group in **IVa** is unsymmetrical, with shorter Fe–C distances of 1.818 Å (B3LYP) or 1.827 Å (BP86) and longer Fe–C distances of 2.143 Å (B3LYP) or 2.078 Å (BP86).

The structure of next lowest energy found for $\text{Cp}_2\text{Fe}_2(\text{CO})$ is a singlet bridged isomer **IVb** far above the global minimum **IVa** at 30.7 kcal/mol (B3LYP) or 25.4 kcal/mol (BP86). The next structure for $\text{Cp}_2\text{Fe}_2(\text{CO})$ above the global minimum **IVa** at 31.3 kcal/mol (B3LYP) or 25.4 kcal/mol (BP86) is the singlet structure **IVc** with a terminal CO group. The Fe–Fe distance in the singlet unbridged structure **IVc** at 2.340 Å (B3LYP) or 2.403 Å (BP86) is ~ 0.112 or 0.206 Å longer than the Fe–Fe distance in the singlet bridged structure **IVb** at 2.228 or 2.197 Å. In **IVc**, one of the C_5H_5 rings (the one on the “bottom” in **IVc**) appears to use two of its C atoms as a bridge between the two Fe atoms. This interpretation is supported by Fe–C bond distances of 2.180 Å (B3LYP) or 2.083 Å (BP86) to one of these bridging Cp C atoms and 2.156 Å (B3LYP) or 1.999 Å (BP86) to the other bridging Cp C atom.

The 18-electron rule requires **IVa** as well as the other $\text{Cp}_2\text{Fe}_2(\text{CO})$ isomers to have an Fe⁴–Fe quadruple bond. In this connection, the Fe–Fe distance of 2.069 Å (B3LYP) or 1.998 Å (BP86) in **IVa** is significantly shorter than the Fe–Fe distance of 2.147 Å (B3LYP) or 2.120 Å in the global minimum of $\text{Cp}_2\text{Fe}_2(\text{CO})_2$ (**IIIa**), where only an Fe=Fe triple bond is required to give both Fe atoms the favored 18-electron configuration.

Table 1. Optimized Geometrical Parameters (Bond Distances in Å and Bond Angles in deg), Total Energy (E in hartrees), and Relative Energy (ΔE in kcal/mol) for $\text{Cp}_2\text{Fe}_2(\text{CO})_4$ Isomers

	Ia (trans dibridged C_3 isomer)			Ib (cis dibridged C_{2v} isomer)			Ic (trans unbridged C_{2h} isomer)	
	B3LYP	BP86	expt.	B3LYP	BP86	expt.	B3LYP	BP86
Fe–Fe	2.570	2.540	2.539 ⁴	2.573	2.545	2.531 ⁵	2.742	2.713
Fe–C _{bridge} ^a	1.926	1.923	1.924	1.928	1.925	1.917		
Fe–C _{terminal} ^a	1.766	1.745	1.761	1.770	1.750	1.745	1.759	1.743
C–O _{bridge} ^a	1.186	1.201	1.180	1.187	1.202	1.180		
C–O _{terminal} ^a	1.163	1.181	1.150	1.160	1.177	1.153	1.165	1.182
C_b –Fe– C_b ^a	94.76	97.32	97.4	95.16	95.99	96.0		
Fe– C_b –Fe	83.74	82.68	82.6	83.72	82.76	82.8		
C_i –Fe– C_b ^a	93.47	93.48	93.8	90.84	90.57	89.0	95.16	94.13
– E	3368.11437	3368.60272		3368.11341	3368.60008		3368.11064	3368.58815
ΔE	0	0	0	0.6	1.7	–1.3	2.3	9.1
imaginary frequency	none	none		46i, 30i	53i, 36i		none	none

^a Average values.

Table 2. Fe–Fe Distances (Å), Total Energy (E in hartrees), Relative Energy (ΔE in kcal/mol), and Imaginary Frequencies for $\text{Cp}_2\text{Fe}_2(\text{CO})_3$ Isomers

	IIa (C_{2v}): 3B_1		IIb (C_s): $^1A'$		IIc (C_{2v}): 3B_2		IId (C_{2v}): 1A_1	
	B3LYP	BP86	B3LYP	BP86	B3LYP	BP86	B3LYP	BP86
Fe–Fe	2.268	2.264	2.459	2.375	2.985	2.736	2.747	2.692
$-E$	3254.73303	3255.21049	3254.71502	3255.19346	3254.67153	3255.12263	3254.66337	3255.13909
ΔE	0	0	11.3	10.7	38.6	55.1	43.7	44.8
imaginary frequency	25i, 23i	25i, 24i	20i	31i	786i, 602i, 56i, 35i	838i, 68i	67i, 32i	67i, 29i

Table 3. Fe–Fe Distances (Å), Total Energy (E in hartrees), Relative Energy (ΔE in kcal/mol), and Imaginary Frequencies for Seven $\text{Cp}_2\text{Fe}_2(\text{CO})_2$ Isomers

		IIIa (C_{2v}): 1A_1	IIIb (C_s): $^3A''$	IIIc (C_{2h}): 1A_g	IIId (C_i): 3A_u	IIIe (C_{2v}): 1A_1	IIIf (C_{2v}): 3B_1	IIIg (C_s): $^3A'$	
				B3LYP	BP86	B3LYP	BP86	B3LYP	BP86
Fe–Fe		2.147	2.329	2.299	2.660	2.407	2.632	2.462	
$-E$		3141.33978	3141.35545	3141.26615	3141.30673	3141.23593	3141.28290	3141.34074	
ΔE		0	−9.8	46.2	20.7	65.2	35.7	−0.6	
imaginary frequency		none	91i, 35i	84i, 66i, 40i	33i	138i, 55i, 36i	132i, 49i, 41i, 24i	334i, 26i, 16i	
		BP86	22i	78i, 73i, 39i	65i		247i, 127i, 92i, 48i	92i	

Table 4. Fe–Fe Distances (Å), Total Energy (E in hartrees), Relative Energy (ΔE in kcal/mol), and Imaginary Frequencies for $\text{Cp}_2\text{Fe}_2(\text{CO})$

	IVa (C_1): 3A		IVb (C_s): $^1A'$		IVc (C_1): 1A	
	B3LYP	BP86	B3LYP	BP86	B3LYP	BP86
Fe–Fe	2.069	1.998	2.228	2.197	2.340	2.403
$-E$	3027.92754	3028.37151	3027.87858	3028.33095	3027.87762	3028.33110
ΔE	0	0	30.7	25.4	31.3	25.4
imaginary frequency	35i	none	5i	44i, 32i	none	none

Table 5. NBO Analysis for the $\text{Cp}_2\text{Fe}_2(\text{CO})_n$ ($n = 4, 3, 2, 1$) Isomers (B3LYP)

isomer	state	no. of COs	no. of bridging COs	Fe–Fe distance (Å)	formal central bond order	Fe natural charge
Ia	$^1A'$	4	2	2.570	1	−0.13
Ib	1A_1	4	2	2.573	1	−0.13
Ic	1A_g	4	0	2.742	1	−0.13
IIa	3B_1	3	3	2.268	2	−0.14
IId	1A_1	3	1	2.747	2	0.06
IIIa	1A_1	2	2	2.147	3	0.06
IIIb	$^3A''$	2	2	2.329	3	0.11
IIIc	1A_g	2	0	2.299	3	0.11
IIId	3A_u	2	0	2.660	3	0.16
IVa	3A	1	1	2.069	4	0.67
IVb	$^1A'$	1	1	2.228	4	0.16
IVc	1A	1	0	2.340	4	0.33
						0.44
						0.44
						0.31
						0.31
						0.15
						0.43

3.2. Structure and Bonding. The Fe–Fe distances in the singlet structures of $\text{Cp}_2\text{Fe}_2(\text{CO})_n$ ($n = 4, 3, 2, 1$) are seen to correlate with the number of bridging CO groups and the formal Fe–Fe bond order required to give both Fe atoms the favored 18-electron configuration (Table 5). Thus, each unit increase in the formal Fe–Fe bond order is predicted to shorten the Fe–Fe bond distances (B3LYP) by roughly 0.2 Å in accordance with the known crystal structures of $\text{Cp}_2\text{Fe}_2(\text{CO})_n$ ($n = 4$ and 3). Similarly, each additional

bridging CO group for a $\text{Cp}_2\text{Fe}_2(\text{CO})_n$ derivative shortens the Fe–Fe bond distances by roughly 0.1 Å.

The triplet global minimum **IIa** (in Figure 3) can be formulated with an Fe=Fe $\sigma + ^2/2\pi$ double bond similar to the O=O double bond in dioxygen with the favored 18-electron configuration for both Fe atoms. Its Fe=Fe distance of 2.268 Å (Table 5) is consistent with the Fe–Fe distances in the singlet $\text{Cp}_2\text{Fe}_2(\text{CO})_n$ derivatives and a lowering of ~ 0.2 Å for each unit of formal bond order and ~ 0.1 Å for each additional bridging CO group. Similarly, the triplet global minimum $\text{Cp}_2\text{Fe}_2(\mu\text{-CO})$ (**IVa** in Figure 5) can be formulated with an Fe⁴–Fe $\sigma + 2\pi + ^2/2\delta$ quadruple bond, which has not yet been found in any isolable molecule. A $\text{Cp}_2\text{Fe}_2(\mu\text{-CO})$ derivative analogous to **IVa** would be an interesting synthetic target, possibly using bulky substituents on the Cp ring to stabilize the binuclear structure and Fe⁴–Fe quadruple bond toward oligomerization to structures of higher nuclearity.

In most cases, the formal Fe–Fe multiple bond orders greater than unity suggested by metal–metal bond distances and 17- or 18-electron Fe electronic configurations as discussed above are significantly higher than the NBO Fe–Fe bond orders (Table 5). This discrepancy increases as the formal metal–metal bond order increases. The use of some of the metal–metal multiple-bond electron density for back- π -bonding to the CO groups is a possible cause for at least some of this discrepancy.

3.3. Dissociation Energies. Table 6 reports the dissociation energies in terms of the single carbonyl dissociation step



The predicted dissociation energy of one CO group from

Table 6. Dissociation Energies (kcal/mol) for the Successive Removal of Carbonyl Groups from Cp₂Fe₂(CO)₄ and Fe₂(CO)₉ (Ref 27)

	B3LYP	BP86
Cp ₂ Fe ₂ (CO) ₄ (Ia) → Cp ₂ Fe ₂ (CO) ₃ (IIa) + CO	33.1	40.8
Cp ₂ Fe ₂ (CO) ₃ (IIa) → Cp ₂ Fe ₂ (CO) ₂ (IIIa) + CO	46.2	51.0
Cp ₂ Fe ₂ (CO) ₂ (IIIa) → Cp ₂ Fe ₂ (CO) (IVa) + CO	52.5	68.2
Fe ₂ (CO) ₉ → Fe ₂ (CO) ₈ + CO	29.4	35.1
Fe ₂ (CO) ₈ → Fe ₂ (CO) ₇ + CO	25.4	37.6
Fe ₂ (CO) ₇ → Fe ₂ (CO) ₆ + CO	32.6	33.9

Cp₂Fe₂(CO)₄ to give Cp₂Fe₂(CO)₃ (Table 6) is 33.1 kcal/mol (B3LYP) or 40.8 kcal/mol (BP86). Further dissociation of a CO group from Cp₂Fe₂(CO)₃ to give Cp₂Fe₂(CO)₂ requires 46.2 kcal/mol (B3LYP) or 51.0 kcal/mol (BP86). The next stage of dissociation of CO from Cp₂Fe₂(CO)₂ to Cp₂Fe₂(CO) requires 52.5 kcal/mol (B3LYP) or 68.2 kcal/mol (BP86). A comparison of CO dissociation from Cp₂Fe₂(CO)₄ and Fe₂(CO)₉ (Table 6) suggests that the energy for dissociation of the first CO group from Fe₂(CO)₉ is similar to that of Cp₂Fe₂(CO)₄.

3.4. Vibrational Frequencies. The harmonic vibrational frequencies and their infrared intensities for all of the structures have been evaluated by the B3LYP and BP86 methods. Complete reports of the vibrational frequencies and infrared intensities are given in the Supporting Information. These results have been used to determine if a structure is a genuine minimum.

The predicted ν(CO) frequencies for the Cp₂Fe₂(CO)_n (n = 4, 3, 2, 1) isomers are of particular interest because any future experimental work to detect such species is likely to rely on the relatively strong ν(CO) frequencies for initial product characterization. The ν(CO) stretching frequencies are listed in Table 7 for all of the Cp₂Fe₂(CO)_n (n = 4, 3, 2, 1) structures studied in this work. In general, the ν(CO) frequencies predicted by the BP86 functional are 60–100 cm⁻¹ lower than those predicted by the B3LYP functional. Furthermore, the ν(CO) infrared frequencies computed with the BP86 functional are in very close agreement (typically within 15 cm⁻¹) with the experimental infrared ν(CO) frequencies in hydrocarbon solvents for (η⁵-C₅H₅)₂Fe₂(CO)₂(μ-CO)₂, (η⁵-C₅H₅)₂Fe₂(μ-CO)₃, and (η⁵-C₅H₅)₂Fe₂(CO)₂ (Table 7). In general, the ν(CO) frequencies of (η⁵-Me₅C₅)₂Fe₂(CO)_n derivatives are ~30 cm⁻¹ lower than those of the corresponding ν(CO) frequencies of the analogous (η⁵-C₅H₅)₂Fe₂(CO)_n owing to the inductive effect of the five methyl groups on the Cp rings.

In transition-metal carbonyl chemistry, the ν(CO) frequencies of typical symmetrical two-electron donor bridging CO groups are well-known to occur 150–200 cm⁻¹ below the ν(CO) frequencies of terminal CO groups in a given type of metal carbonyl derivative. This same trend is found for the Cp₂Fe₂(CO)_n (n = 4, 3, 2, 1) derivatives studied in this work, where the bridging ν(CO) frequencies fall in the range of 1828–1796 cm⁻¹ and the terminal ν(CO) frequencies fall in the range of 1991–1897 cm⁻¹ (BP86). Similar observations concerning bridging and terminal ν(CO) frequencies were made in our previous work with Cp₂Co₂(CO)_n (n = 3, 2, 1) derivatives.²⁸

The ν(CO) frequencies computed for the Cp₂Fe₂(CO)₂ isomers (Table 7) are consistent with the experimental work

Table 7. Metal Carbonyl ν(CO) Frequencies (in cm⁻¹) Predicted for the Cp₂Fe₂(CO)_n (n = 4, 3, 2, 1) Isomers (Infrared Intensities in Parentheses and in km/mol; Infrared Active Frequencies Given in Bold Type)

	B3LYP	BP86	exptl ¹⁷	
<i>trans</i> -Cp ₂ Fe ₂ (CO) ₄ Ia (C _s)	2051 (a', 34)	1961 (a', 37)		
	2037 (a', 1480)	1946 (a', 1210)	1962	
	1901 (a', 0)	1820 (a', 0)		
	1858 (a'', 1120)	1796 (a'', 860)	1794	
<i>cis</i> -Cp ₂ Fe ₂ (CO) ₄ Ib (C _{2v})	2079 (a₁, 1430)	1991 (a₁, 1150)	2006	
	2042 (b₂, 185)	1956 (b₂, 199)	1962	
	1898 (a ₁ , 4)	1819 (a ₁ , 3)		
	1857 (b₁, 1130)	1795 (b₁, 860)	1794	
<i>trans</i> -Cp ₂ Fe ₂ (CO) ₄ Ic (C _{2h})	2057 (a _g , 0)	1973 (a _g , 0)		
	2016 (a_u, 1500)	1931 (a_u, 1240)		
	2013 (b_u, 1270)	1947 (b_u, 930)		
	1999 (b _g , 0)	1918 (b _g , 0)		
Cp ₂ Fe ₂ (CO) ₃ IIa (C _{2v})	1951 (a ₁ , 0)	1862 (a ₁ , 0)		
	1905 (a₁, 1010)	1820 (a₁, 800)	1811	
	1904 (b₁, 980)	1819 (b₁, 780)		
Cp ₂ Fe ₂ (CO) ₃ IIb (C _s)	1880 (a', 29)	1807 (a', 77)		
	1842 (a'', 1160)	1781 (a'', 920)		
	2047 (a', 830)	1949 (a', 550)		
Cp ₂ Fe ₂ (CO) ₃ IIc (C _{2v})	2042 (a₁, 1180)	1949 (a₁, 950)		
	1975 (b₂, 363)	1890 (b₂, 232)		
	1796 (a₁, 540)	1730 (a₁, 438)		
Cp ₂ Fe ₂ (CO) ₂ IIIa (C _{2v})	1939 (a₁, 202)	1851 (a₁, 195)		
	1918 (b₁, 1210)	1828 (b₁, 900)		
	IIIb (C _s)	1918 (a', 100)	1820 (a', 89)	
		1901 (a'', 1240)	1798 (a'', 960)	
	IIIc (C _{2h})	2013 (a _g , 0)	1920 (a _g , 0)	
		1988 (b_u, 2620)	1904 (b_u, 2030)	
IIId (C _i)	2015 (a _g , 0)	1919 (a _g , 0)		
	1998 (a_u, 2540)	1897 (a_u, 2330)		
	2049 (a₁, 1590)	1951 (a₁, 1290)	1958	
Cp ₂ Fe ₂ (CO) IVa (C ₁)	1976 (b₂, 404)	1905 (b₂, 367)	1904	
	1949 (830)	1864 (640)		
	1894 (a', 630)	1789 (a', 474)		
IVc (C ₁)	1987 (1430)	1908 (1080)		

by Vitale, Archer, and Bursten¹⁷ (VAB) on the photolysis of *trans*-Cp₂Fe₂(CO)₂(μ-CO)₂ (**Ia**) in soft hydrocarbon matrices at low temperatures to generate Cp₂Fe₂(CO)₂ isomers via the triplet **IIa** intermediate. The ν(CO) frequencies (Table 7) of 1951 and 1905 cm⁻¹ (BP86) that we predict for triplet *cis*-Cp₂Fe₂(CO)₂ (**IIIc**) with all terminal CO groups agree well with their experimental values of 1958 and 1904 cm⁻¹, which VAB assign to a triplet isomer similar to **IIIc**. VAB also find evidence for methylated derivatives of the most stable Cp₂Fe₂(CO)₂ isomer, namely, singlet Cp₂Fe₂(μ-CO)₂ (**IIIa**), for which the BP86 functional predicts infrared ν(CO) frequencies at 1851 and 1828 cm⁻¹, with the lower of these frequencies predicted to be more intense than the higher frequency by a factor of about 5 (Table 7). VAB thus observed infrared bands at 1833 and 1812 cm⁻¹ at late stages of the low-temperature photolyses of (η⁵-Me₅C₅)₂Fe₂(CO)₂(μ-CO)₂ and (η⁵-Me₅C₅)(η⁵-C₅H₅)Fe₂(CO)₂(μ-CO)₂, respectively, in hydrocarbon matrices. These infrared bands can be assigned to the most intense bridging CO frequency of the corresponding singlet **IIIa** isomers (Figure 4) after some adjustment for the inductive effects of multiple methyl ring substituents, which lower the ν(CO) frequencies.

4. Summary

The *trans*- and *cis*-Cp₂Fe₂(CO)₂(μ-CO)₂ isomers of Cp₂Fe₂(CO)₄ known experimentally are predicted by DFT

(28) Wang, H.; Xie, Y.; King, R. B.; Schaefer, H. F. *J. Am. Chem. Soc.* **2005**, *127*, 11646.

methods to be genuine minima with no significant imaginary vibrational frequencies. The energies of these two $\text{Cp}_2\text{Fe}_2(\text{CO})_2(\mu\text{-CO})_2$ structures are very similar, consistent with the experimental observation of an equilibrium between these isomers in solution. An intermediate between the interconversion of the *trans*- and *cis*- $\text{Cp}_2\text{Fe}_2(\text{CO})_2(\mu\text{-CO})_2$ dibridged isomers of $\text{Cp}_2\text{Fe}_2(\text{CO})_4$ can be the *trans* unbridged isomer of $\text{Cp}_2\text{Fe}_2(\text{CO})_4$ calculated to be 2.3 kcal/mol (B3LYP) or 9.1 kcal/mol (BP86) above the global minimum *trans*- $\text{Cp}_2\text{Fe}_2(\text{CO})_2(\mu\text{-CO})_2$. For the unsaturated $\text{Cp}_2\text{Fe}_2(\text{CO})_3$, the known triplet isomer $\text{Cp}_2\text{Fe}_2(\mu\text{-CO})_3$ with an $\text{Fe}=\text{Fe}$ double bond similar to the $\text{O}=\text{O}$ double bond in O_2 is found to be the global minimum. The lowest-energy structure for the even more unsaturated $\text{Cp}_2\text{Fe}_2(\text{CO})_2$ is a dibridged structure $\text{Cp}_2\text{Fe}_2(\mu\text{-CO})_2$, with a short Fe–Fe distance suggestive of the $\text{Fe}\equiv\text{Fe}$ triple bond required to give both Fe atoms the favored 18-electron configuration. Singlet and triplet unbridged structures for $\text{Cp}_2\text{Fe}_2(\text{CO})_2$ were also found but at energies considerably higher (20–50 kcal/mol) than those of the

global minimum $\text{Cp}_2\text{Fe}_2(\mu\text{-CO})_2$. The lowest-energy structure for $\text{Cp}_2\text{Fe}_2(\text{CO})$ is the triplet unsymmetrically bridged structure $\text{Cp}_2\text{Fe}_2(\mu\text{-CO})$, with a short Fe–Fe distance suggestive of the $\sigma + 2\pi + 2/2\delta$ $\text{Fe}^4\text{-Fe}$ quadruple bond required to give both Fe atoms the favored 18-electron rare gas configuration.

Acknowledgment. We are grateful to the National Science Foundation for support of this work under Grant CHE-0209857. H.W. thanks the China Scholarship Council for financial support (CSC Grant No. 2003851025) and the National Natural Science Foundation of China (Grant No. 10276028).

Supporting Information Available: Complete tables of harmonic vibrational frequencies for $\text{Cp}_2\text{Fe}_2(\text{CO})_n$ ($n = 4, 3, 2, 1$) isomers (Tables S1–S17) and the 17 $\text{Cp}_2\text{Fe}_2(\text{CO})_n$ ($n = 4, 3, 2, 1$) structures discussed in this paper (Figure S1). This material is available free of charge via the Internet at <http://pubs.acs.org>.

IC051613L